

Figure 4. Images of normal liver. (a) Unenhanced CT scan, (b) HPI image, (c) arterial perfusion image, and (d) portal perfusion image.

ment disease extent before chemotherapy.

Figure 6 demonstrates an unenhanced CT scan and the corresponding perfusion images. The metastasis has high values on the HPI image but low values on the portal perfusion image. The perfusion is also abnormal in the areas that do not appear to contain metastases on the conventional CT image, with an increase in HPI (0.4–0.55) and arterial perfusion (0.6–0.85 mL/min/mL).

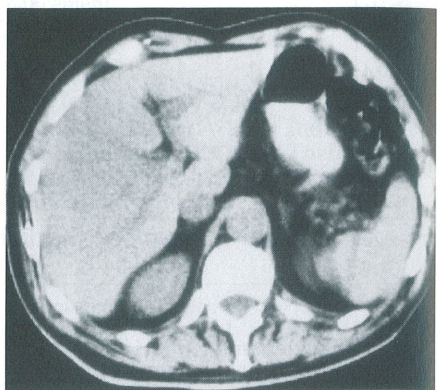
DISCUSSION

To our knowledge, the quantification of hepatic arterial and portal perfusion with dynamic CT with creation of functional images has not been previously described. Although dynamic CT has been used for evaluation of tissue perfusion (3,10–14), including functional imaging (4,15,16), these techniques have not been systematically applied to the liver and would not allow differentiation of arterial and portal phases. Partanen (17) has described differences in TDCs between normal and cirrhotic livers, but again the frequency of data acquisition was too low for differentiation of arterial and portal phases.

The statistically significant correlation between dynamic colloid scintigraphy and dynamic CT has provided reasonable direct validation of the CT technique for determining the HPI. Portal perfusion is underestimated with the CT method because there is some loss of contrast medium into the extracellular space of the spleen and gut during its first pass through these organs before passage to the liver in the portal blood. Thus, CT values for HPI are generally higher than the corresponding HAR values from scintigraphy.

The fact that the CT technique has demonstrated changes in liver perfusion parameters in disease states provides further clinical validation and indicates potential clinical uses of the technique. The increase in HPI that occurs in cirrhosis is due to not only a decrease in portal perfusion as a result of portal hypertension but also to a rise in arterial perfusion (Fig 1). This reciprocal relationship has been previously demonstrated with use of flow meters in an experimental dog model (18) and in a human at surgery (19) and has been suggested as the mechanism for transient regional variations in liver attenuation after intra-vascular administration of contrast medium in portal vein branch thrombosis and focal liver lesions (20–23).

Liver tumors, whether primary hepatocellular carcinoma or metastatic deposits, have a blood supply derived almost exclusively from the arterial rather than portal circulation and, hence, appear as areas of increased HPI on the functional images. As would be expected, measured perfusion was higher in the hepatocellular carcinomas than in the metastases with this CT technique. In livers that contain metastases, the areas that appear morphologically unaffected display abnormal hemodynamics, with an increase in arterial perfusion and HPI. There are many possible explanations for this. Radionuclide studies of liver blood flow in patients with colonic cancer have demonstrated a group of patients with an increased HPI in whom metastases were not visible on images or at surgery (24). Such patients have a greater probability of subsequently developing hepatic metastases than do those with normal flow characteristics, and it is proposed that the presence of "micrometastases" (eg, metastases too small



a.

to visualize) causes alterations in liver hemodynamics. Thus, in patients with visible metastases, the apparently unaffected portions of liver could contain micrometastases. A further explanation would be, as postulated by Itai et al (20) for transient lobar attenuation differences in patients with focal liver lesions, that the presence of a hypervascular lesion within a region of the liver increases the arterial flow not just to the lesion itself but to the whole of that liver region as a result of a steal phenomenon. Alternatively, increasing pressure within a liver segment or lobe containing metastases may reduce portal flow to that portion of liver with a reciprocal rise in arterial perfusion.

Other methods that allow separate evaluation of arterial and portal flow within the liver include dynamic colloid scintigraphy, Doppler US, and magnetic resonance (MR) imaging. As discussed earlier, scintigraphy cannot accurately demonstrate regional variations in flow parameters or depict the left lobe. Furthermore, although the arterial/total flow ratio can be obtained, arterial and portal components cannot be quantified separately. Doppler US is largely limited to evaluating large and medium-size vessels and, thus, the ability to demonstrate regional variations is limited to perhaps left and right hepatic arteries

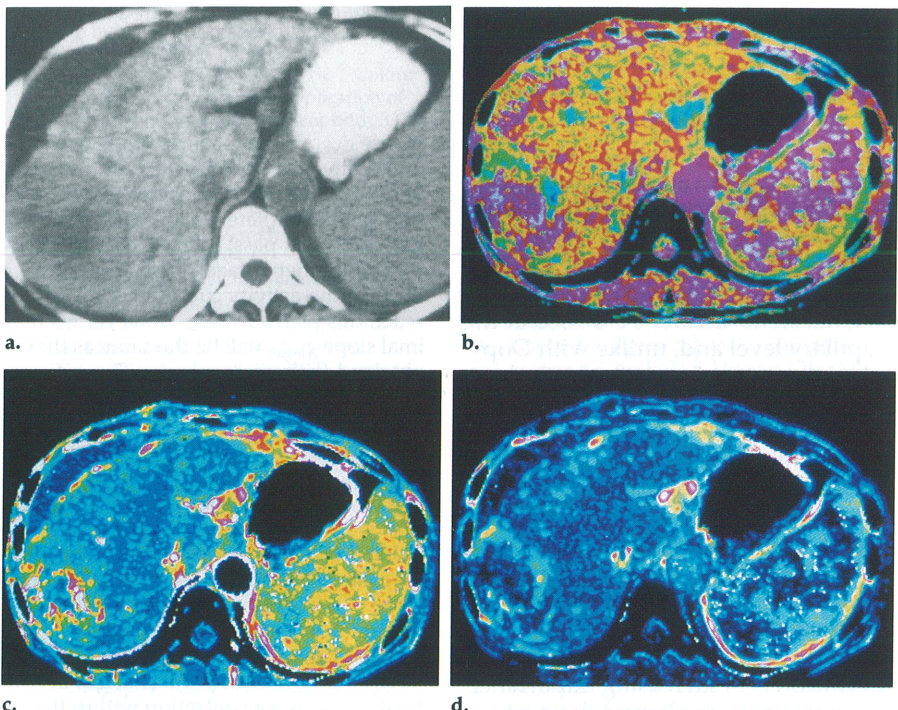


Figure 5. Idiopathic cirrhosis with hepatocellular carcinoma. (a) Unenhanced CT scan, (b) HPI image, (c) arterial perfusion image, and (d) portal perfusion image. The HPI is elevated throughout the liver. Note the high arterial perfusion in the periphery of the tumor, with lower values in the necrotic center.

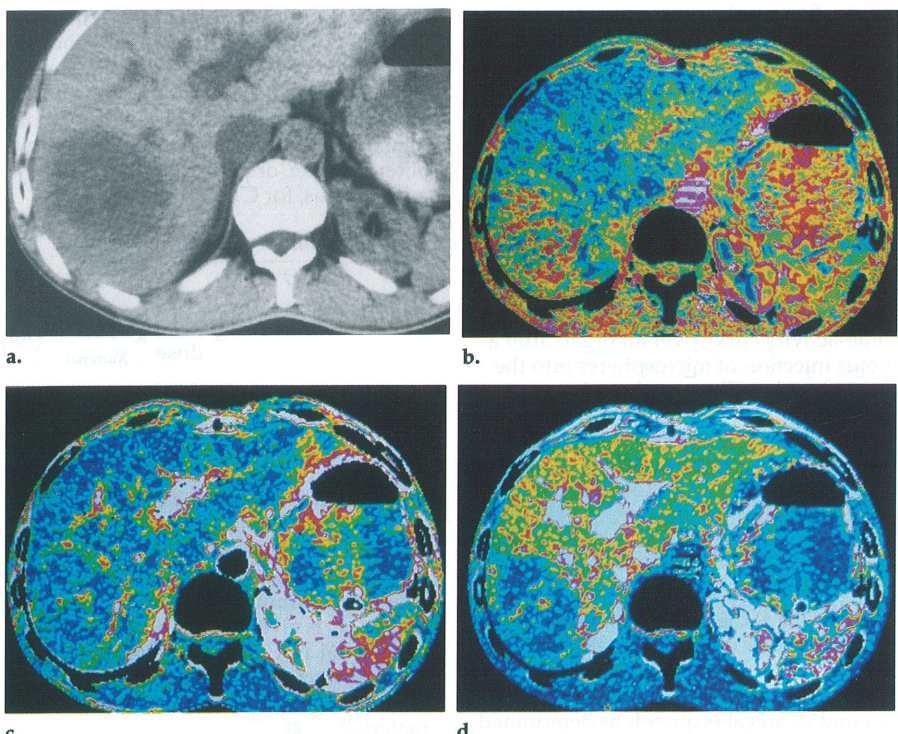


Figure 6. Hepatic metastasis. (a) Unenhanced CT scan, (b) HPI image, (c) arterial perfusion image, and (d) portal perfusion image. Note high arterial and low portal perfusion in the metastasis in the right lobe. The remainder of the liver also demonstrates an increased HPI.

and portal veins. Doppler studies primarily provide measurement of blood velocity, and conversion to the more physiologically important volume flow adds substantial inaccuracies.

The CT technique benefits from assessing perfusion at the capillary level, which is more directly related to the metabolic requirements of the tissue than the flow in the supplying

vessel. Ultimately, MR imaging techniques may be developed to address these problems.

The main limitation of the CT technique is that only one section level can be readily studied. Thus, although regional variations in the axial plane can be studied, craniocaudal variations may be missed. In addition, the radiation burden of the technique is not inconsiderable; this prevents a greater frequency of data acquisitions (which is technically possible with the Somatom Plus unit). The sequence of data acquisitions used in this study was chosen as a compromise between sample frequency and radiation exposure. After an initial pause to allow passage of contrast material through the heart and lungs, the interval between acquisitions is shorter early in the sequence when changes in enhancement are occurring most rapidly, with greater spacing later when changes occur at a lower rate.

The greatest potential source of error is patient movement during the single-location sequence; this prevented analysis in one patient. Structures with higher or lower attenuation values moving into and out of the section under study between acquisitions alter the recorded attenuation values because of the varying partial-volume effect. The sensation of flushing caused by the injection of the bolus of contrast medium is particularly prone to cause patient movement. This can be minimized by using low-osmolarity agents and carefully instructing the patient and, in practice, rarely degrades the functional images to any extent.

When generating TDCs from very small regions or individual pixels, photon noise becomes an important consideration. Random variations in photon numbers and detector response cause variability in measured attenuation values and, hence, errors in the calculated perfusion values. Use of a soft-tissue reconstruction algorithm (low noise) and compression of the data into a 256×256 matrix reduce this effect while maintaining good spatial resolution. We have evaluated this effect by performing dynamic CT in a water phantom. The error in the perfusion measurements depends on the value of perfusion itself; the error is greater with low perfusion. With the Somatom Plus unit, the error resulting from photon noise for an individual pixel (256×256) with a typical perfusion value of 0.32 mL/min/mL is $\pm 0.06 \text{ mL/min/mL}$. For perfusion values from a larger ROI (eg, 50 or more pixels as